Selective and diagnostic labelling of serine hydrolases with reactive phosphonate inhibitors†

Harmen P. Dijkstra,*[a] Hein Sprong,[b] Bas N. H. Aerts,[a] Cornelis A. Kruithof,[a] Maarten R. Egmond[b] and Robertus J. M. Klein Gebbink*[a]

Received 9th November 2007, Accepted 29th November 2007
First published as an Advance Article on the web 17th December 2007
DOI: 10.1039/b717345h

Reactive phosphonates are important probes to target the active site of serine hydrolases, one of the largest and most diverse family of enzymes. Developing such inhibitory probes is of special importance in activity based protein profiling, a strategy that is increasingly used to gain information about a certain class of enzymes in complex proteosomes. Therefore, gaining detailed information about these inhibition events on the individual protein level is important since it affords information that can be used to fine-tune the probe for a specific task. Here, we report a novel and versatile synthesis protocol to access a variety of functionalised *p*-nitrophenyl phosphonate (PNPP) inhibitors from a common azide functionalised precursor using click chemistry. The obtained PNPPs were successfully used to covalently label serine hydrolases in their active sites with molecular tags. Furthermore, a model study is described in which we developed straightforward protocols that can be used to study protein inhibition events. Kinetic studies using UV–Vis and fluorescence spectroscopy techniques revealed that these PNPPs possess different inhibition rates for various proteins and were shown to be suitable probes to discriminate between various lipases. Additionally, we demonstrate that PNPPs are highly selective for serine hydrolases, making these probes very interesting as diagnostic or affinity probes for studying proteins in complex proteosomes.

Introduction

Proteins play a crucial role in regulating many complex biological mechanisms. Using classical biological analysis techniques, *e.g.* sequencing and crystallographic techniques, the structures of many of these proteins have been elucidated. Despite these achievements, studying the specific function of proteins in their natural environment remains difficult due to the complex post-translational events[1] by which proteins are regulated. In search for more direct methods to study proteins, the field of proteomics has produced some valuable techniques, such as LC-MS/MS to study protein modification[2] and protein microarrays to study the natural activities of proteins.[3] Although these methods have provided detailed information about protein expression and interactions and *in vitro* functioning of proteins, they are not suitable for studying protein function in cells or tissue. Therefore new methods in which chemical and biological techniques are combined have been developed in order to (chemoselectively) modify proteins for the purpose of studying their function in complex biological media.[4] Especially native chemical ligation (NCL)[5] and expressed protein ligation (EPL)[6] have been intensively applied in this research field. Also alternative chemical biological methods that use small molecules for covalent linking to target proteins, thereby creating the potential of studying these proteins in their natural environment, were reported.[7] A recent and highly interesting strategy in this area is the covalent, selective modification of the active site of proteins by small molecule inhibitors, a technique called activity-based protein profiling (ABPP).[8] This technique not only labels proteins in an efficient and potentially selective manner, it also knocks out the natural activity of proteins, an event that can give valuable information about protein function. Additionally, since the active site is targeted, this protocol can potentially also discriminate between different classes of proteins or even individual proteins. By decorating the inhibitors with diagnostic or affinity tags, selective protein isolation and analysis has become more straightforward.

Reactive phosphonate inhibitors (Fig. 1) have been successfully applied in the field of ABPP to covalently modify members of the serine hydrolase superfamily with molecular tags, *e.g.* fluorescent groups and biotin.[8–10] Cravatt and co-workers reported the use of functionalised fluorophosphonates (LG = F) as potent inhibitors for serine hydrolases. They demonstrated that ABPP is a suitable technique to label specific proteins in complex proteomic mixtures with diagnostic and/or affinity tags in order to gather information about the active site and function of unexplored or even unknown proteins.[11] Hermetter and co-workers have reported on the use of *p*-nitrophenyl (PNP) phosphonates (LG = *p*-nitrophenol) as irreversible ABPP-inhibitors for lipases and esterases.[10a,b] They extended this technology to develop microarrays for the identification and characterisation of novel and unknown lipolytic enzymes.[10c] Recently, we reported on the selective introduction of

[a]*Chemical Biology & Organic Chemistry, Department of Chemistry, Faculty of Science, Utrecht University, Padualaan 8, 3584 CH, Utrecht, The Netherlands. E-mail: h.p.dijkstra@uu.nl, r.j.m.kleingebbink@uu.nl.; Fax: +31 (0)30 252 3615; Tel: +31 (0)30 253 1889/3120*
[b]*Membrane Enzymology, Department of Chemistry, Faculty of Science, Utrecht University, Padualaan 8, 3584 CH, Utrecht, The Netherlands*

† Electronic supplementary information (ESI) available: ESI-MS data of the various protein constructs and fluorescence spectroscopy data as indicated in the text. See DOI: 10.1039/b717345h

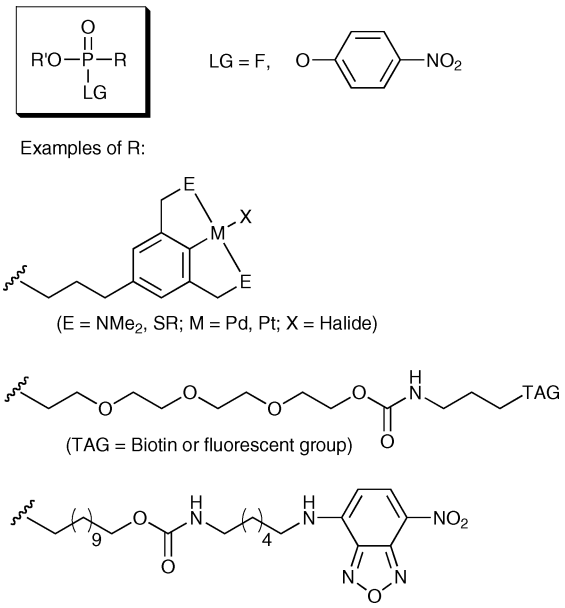

Fig. 1 Examples of reactive phosphonates.

organometallic pincer fragments into the active site of cutinase, a 20 kDa member of the lipase family, using a functionalised PNP phosphonate.[12] The organometallic probes have great potential as diagnostic and affinity tags in protein profiling and as phasing probes in protein crystal structure elucidation.[13]

Serine hydrolases constitute a large superfamily of enzymes and are responsible for many hydrolysis reactions in nature, *e.g.* esterifications, amidations and acyltransfer. As outlined in Scheme 1 for lipases (a subfamily of serine hydrolases), reaction of reactive phosphonates with an enzyme results in protein–inhibitor complexes in which the phosphorous atom binds in a tetrahedral manner, with the P=O binding in the oxy-anion hole. This tetrahedral orientation closely resembles the hydrolysis transition state for the fatty-acid ester hydrolysis, a reaction readily catalysed by lipases. Since these phosphonates react irreversibly and stoichiometrically with serine hydrolases they are powerful probes to isolate, characterise and study serine hydrolases.

We are particularly interested in studying in detail the interaction between a protein and an inhibitor since this is the crucial step in ABPP and little to no information is available about the factors that play a role in these events. Here we demonstrate how novel PNP phosphonate inhibitors can be used to selectively and covalently modify serine hydrolases in an active site-directed manner and how UV–Vis and fluorescence spectroscopy can be used to efficiently monitor the inhibition event. Additionally, we report a new straightforward synthesis protocol for functionalised phosphonate inhibitors in which click chemistry is used to conveniently attach various desired functionalities in the final step to a PNP phosphonate building block.

Results and discussion

Synthesis of PNP phosphonate probes

Reactive phosphonates contain a good leaving group (LG) attached to the electrophilic P-atom, rendering these P–LG bonds very reactive towards a nucleophilic serine in the active site of proteins but also to other (even weak) nucleophiles. Therefore, in the synthesis of these probes extra care has to be taken to prevent cleavage of this bond, as it is crucial to its biological activity. In our studies we focussed on PNP phosphonate (PNPP) inhibitors since the PNP leaving group appeared to be an ideal probe to study the interaction between a selected serine hydrolase and a functionalised PNPP inhibitor (*vide infra*). Preferentially, a general synthesis protocol for phosphonate inhibitors should fulfil a few criteria: (1) the synthetic route should be straightforward without tedious work-ups and consist of only a few steps; (2) the desired tag (R, Fig. 1, *e.g.* diagnostic and affinity tags) should be introduced in the final step in order to get fast access to a variety of functionalised inhibitors and (3) the final coupling step should be mild and tolerate many functionalities. Since such protocols are lacking for PNPP inhibitors, we decided to explore possible synthesis routes that fulfil these criteria. In this study we decided to keep the ethyl group (R′ = Et, Scheme 1) attached to the phosphonate moiety constant whereas the group R can be changed at will depending on the desired functionality needed for protein study/isolation. For the final step in which the tag-functionality will be introduced we have chosen to use the well-known click reaction, a 3 + 2 cycloaddition reaction between an azide and an acetylene in the presence of a copper(I) catalyst affording a triazole heterocycle. This reaction tolerates many sensitive functionalities and is thus expected to leave the

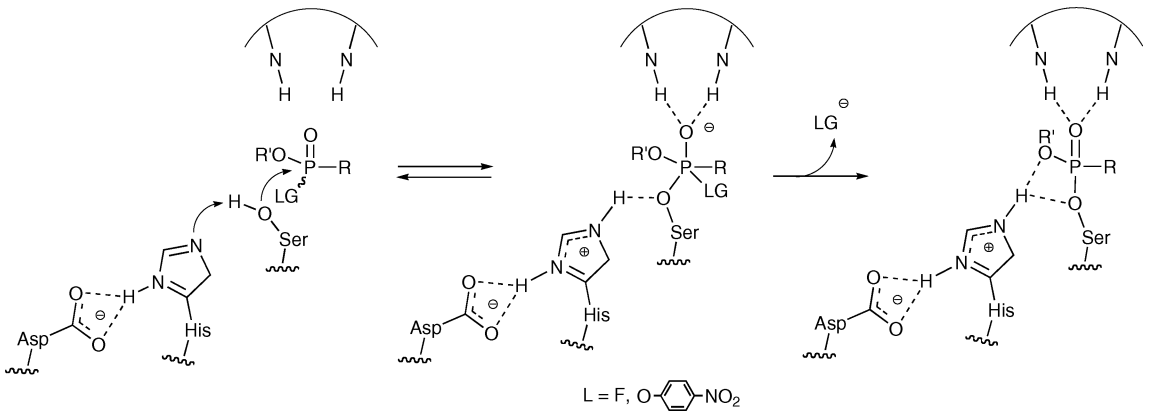

Scheme 1 Proposed mechanism for lipase inhibition by reactive phosphonates.

P–LG bond intact. Moreover, the click reaction can also be used to chemically modify proteins by decorating a protein first with one of the click functionalities followed by a reaction with a tag containing the complementary click functionality.[14] This copper(I) catalysed reaction even proceeds in complex proteomic mixtures. Thus, with this click-chemistry strategy, the tag potentially can be introduced prior to or after the protein inhibition event, making this route very versatile and general.

Our new synthetic route for the functionalised PNPP inhibitors is outlined in Scheme 2. In the first step commercially available 2-(1-bromoethyl)-diethylphosphonate is treated with azide amberlite-resin in DMF giving a nucleophilic replacement of the bromide for an azide functionality. Next, azide phosphonate derivative **1** is treated with excess oxalyl chloride in diethyl ether to afford the moisture sensitive chlorophosphonate **2**. Due to the sensitive nature of the P–Cl bond, this compound was only analysed by NMR spectroscopy to determine full conversion of **1** into **2**. When full conversion was obtained all volatiles were removed and **2** was immediately treated with *p*-nitrophenol (PNP) in benzene in the presence of triethylamine, affording common azide PNP phosphonate intermediate **3** in 41% overall yield from 2-(1-bromoethyl)diethylphosphonate. Thus, compound **3** was synthesised in only 3 steps in gram scale quantities, is air and moisture stable and is easy to handle.

Azide intermediate **3** was explored in the click reaction with various functionalised acetylenes and turned out to be an excellent precursor to access a variety of functionalised phosphonate inhibitors. In Fig. 2 three selected phosphonate inhibitors are depicted that were prepared in this study. Two different tags are depicted: a fluorescent dansyl tag (**4a**) that can potentially be used to study the protein–inhibitor construct using fluorescent spectroscopy, and a biotin moiety (**4b**) that may serve as an affinity tag to isolate proteins using (strept)avidine columns. To illustrate the versatility of this protocol, we also prepared bisphosphonate inhibitor **4c** that has the potential to cross-link proteins. All products were obtained using standard click chemistry conditions ([Cu(MeCN)$_4$BF$_4$], 2,6-lutidine in MeCN)[15] in near quantitative yields using the appropriately propargyl-functionalised dansyl, biotin and triethyleneglycol precursors, respectively. No hydrolysis of the P–OPNP bond was observed, showing the excellent functional group tolerance of the click reaction, making this a convenient protocol to access a variety of reactive phosphonates.

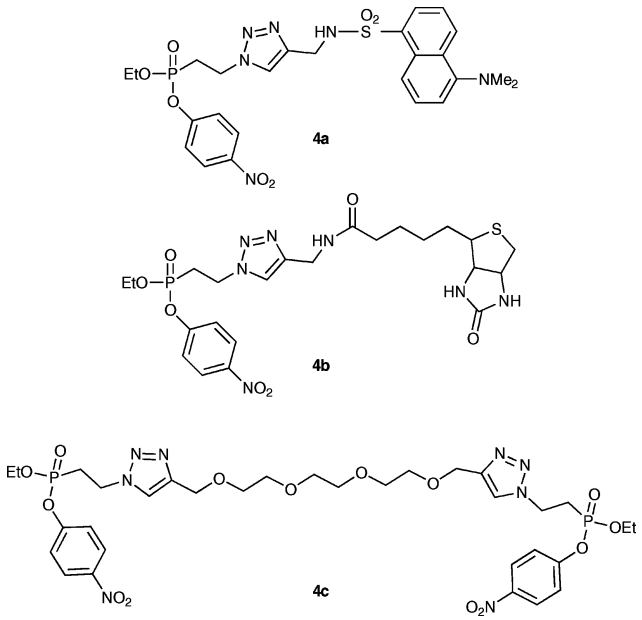

Fig. 2 New functionalised PNPP inhibitors.

Monitoring protein inhibition

As mentioned earlier, reactive phosphonates similar to **3** and **4** were reported to be covalent inhibitors for lipases and esterases.[10,12] The nucleophilic serine-OH in the active site of these enzymes attacks the phosphorus atom of the phosphonate inhibitor, a process in which PNP is released (LG, Scheme 1). Since this process blocks the natural activity of the corresponding protein, this methodology is referred to as active-site directed inhibition and is the crucial step in ABPP. Although it has been reported that reactive phosphonates react at different rates with serine hydrolases (using fluorophosphonates),[11b] no studies were performed on individual proteins that could shine light on the factors that are responsible for the differences in inhibition rate. Especially in the field of protein diagnosis and isolation from complex proteomic mixtures using ABPP, gathering information about the inhibition event of individual proteins is of great value since it ultimately can be used to fine-tune the outcome of these experiments. In this study we decided to study several individual enzymes in our attempt to develop straightforward techniques to study the

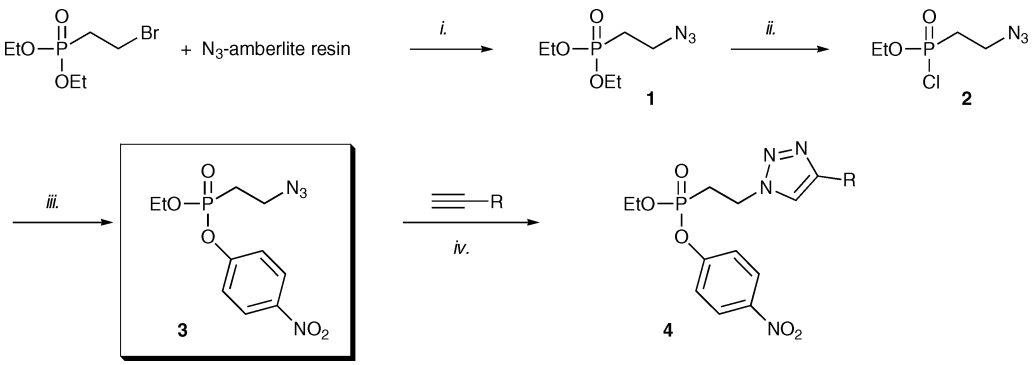

Scheme 2 *i.* DMF, RT, 20 h, 74%; *ii.* oxalyl chloride, Et_2O, RT, 24 h, 95%; *iii.* *p*-nitrophenol, Et_3N, C_6H_6, RT, 3 h, 64%; *iv.* [Cu(MeCN)$_4$BF$_4$], 2,6-lutidine, MeCN, RT, 12 h, >90%.

interaction of these enzymes with our PNPP probes. For this purpose, we initially selected three lipases, *i.e.* cutinase, *Candida antarctica* lipase B (CALB) and *Chromobacterium viscosum* lipase (CVL). We were particularly interested in the inhibition rates of these enzymes when treated with PNPP inhibitors **4** since this would provide valuable information about the accessibility of the active sites of these proteins. The leaving group in this protocol, *i.e.* PNP, is brightly yellow coloured in solution at the inhibition conditions (50 mM tris, 0.1% triton buffer, pH 8.0) and therefore the release of PNP in solution can be conveniently monitored with UV–Vis spectroscopy. Since the reaction between a lipase and a PNP phosphonate inhibitor is stoichiometric, the rate of PNP release is a direct measure of the inhibition rate and thus of the accessibility of the active site. We were also interested to see whether the fluorescent properties of the dansyl group (**4a**) could be used to gather more detailed information about the active site of these proteins. Therefore, we set out a number of inhibition studies with these lipases using various inhibitors and demonstrate how UV–Vis and fluorescence spectroscopy techniques can be used to get insight into the factors that influence the selectivity and efficiency of protein inhibition.

Initially, we started with cutinase (the N172K mutant) since this lipase is well studied and has some attractive features making it an ideal candidate for proof-of-concept studies.[16] Cutinase is a lipase that is lacking the polypeptide lid, commonly observed in the family of lipases, covering the active site. As a consequence the active site of cutinase is readily solvent exposed. Due to these features covalent inhibition of cutinase using reactive phosphonate inhibitors should be straightforward. Indeed, cutinase (typically 25–125 μM) was conveniently labelled with **3**, **4a** and **4b** in an active site-directed manner by mixing cutinase in a tris–triton buffer at pH 8.0 with an excess (typically 5–8 fold) of the appropriate inhibitor and allowing the reaction to proceed to completion within a certain time period. These inhibition times were determined by monitoring the PNP release using UV–Vis analysis. In addition to the PNP release we also performed a control experiment to verify full inhibition by adding aliquots of the inhibition solution to a solution containing *p*-nitrophenyl butyrate (Scheme 3). Lipases are known to hydrolyse the ester bond of aliphatic PNP-esters, *e.g.* PNP butyrate, and thus monitoring the residual lipase activity in this activity assay is a direct measure for the amount of protein inhibition. These experiments demonstrated that the inhibition rate greatly depended on the inhibitor with **3** > **4b** > **4a**. This behaviour is fully attributed to the increased steric bulk at the phosphonate moiety of the inhibitors going from **3** → **4b** → **4a** and is in agreement with our earlier reported results.[12] Fig. 3 shows the representative graphs for the reaction of cutinase with **4a** and clearly illustrates that the data obtained from the inhibition experiment and from the activity control assay result in the similar reaction profiles. The inhibition event followed first order kinetics, giving an inhibition rate constant

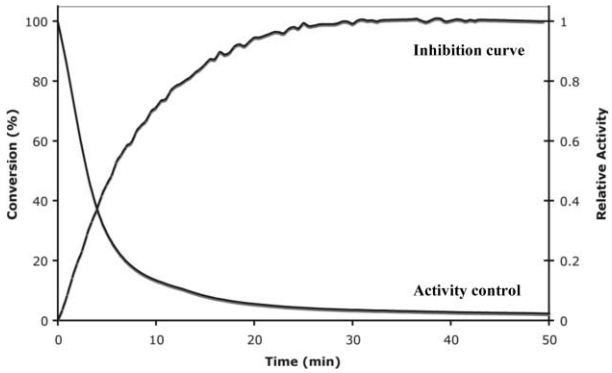

Fig. 3 Typical inhibition and activity control curves.

(k) for cutinase with **4a** of 0.13 min^{-1}. After full inhibition was obtained, the cutinase–inhibitor constructs were purified by dialysis using 150 mM NH_4OAc buffer. The purified cutinase–inhibitor constructs (~25 μM) were subsequently analysed by ESI-MS spectrometry, revealing the formation of the desired cutinase–inhibitor constructs; Mw(cutinase N172K) = 20619 Da, Mw(cutinase-**3**) = 20781 Da, Mw(cutinase-**4a**) = 21070 Da and Mw(cutinase-**4b**) = 21063 Da (see also ESI†).

After successful inhibition of cutinase with our PNPPs we decided to extend this research to other lipases, *i.e. Candida antarctica* lipase B (CALB) and *Chromobacterium viscosum* lipase (CVL). CALB and CVL are two well-studied lipases with high esterase activity in the hydrolysis of PNP-butyrate (Scheme 3).[17] For these experiments we only used dansyl inhibitor **4a** since it allows us to perform additional analyses using fluorescence spectroscopy. Treatment of CALB and CVL with **4a** (8 equivalents) resulted in full inhibition of both lipases according to the PNP release and the activity control assay. Similar data as shown for cutinase (Fig. 3) were obtained. It was found that CALB ($k = 0.66\ min^{-1}$) possesses even higher first order inhibition rates than cutinase ($k = 0.13\ min^{-1}$) with **4a** whereas CVL ($k \ll 0.01\ min^{-1}$) inhibition was much slower. The remarkable difference in inhibition rates, as found here within the subfamily of lipases, can be explained by comparing reported crystal structures of all three lipases.[18] The crystal structures clearly reveal that the active site of CVL is buried much deeper inside the protein than the active sites of cutinase and CALB. As a consequence a considerable amount of steric hindrance occurs during the inhibition reaction of CVL. These experiments demonstrate how specially designed reactive phosphonates in combination with a simple analysis technique can be used to conveniently access information about the active site of proteins, both qualitatively and quantitatively.

Fluorescence spectroscopy studies

Also for CALB-**4a** and CVL-**4a** we attempted to acquire ESI-MS data of the protein–inhibitor constructs. Unfortunately, after

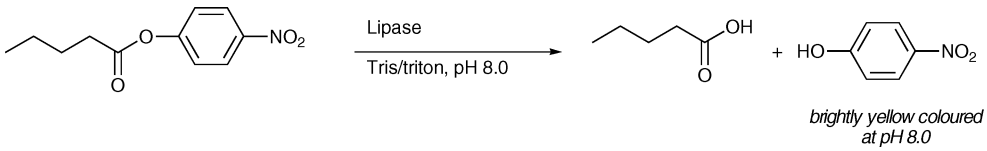

Scheme 3 Activity control test.

purification by dialysis, no satisfactory ESI-MS data could be obtained, probably due to (poly)glycosylation of the proteins as only small glycol fragments were observed. Therefore, we decided to study the protein–**4a** constructs in more detail by fluorescence spectroscopy in order to confirm the presence of the dansyl group in the protein–inhibitor construct. Typically, a 2.5 μM solution of a dialysed protein–**4a** construct in 150 mM NH_4OAc buffer was excited at 340 nm (the maximum absorption wavelength of the dansyl group) and the emission is measured from 400–560 nm (Fig. 4). Free **4a** in the same buffer was measured as a control. In all fluorescence experiments also the native proteins without inhibitors were measured as controls (data not shown) and in all cases no emission between 400–560 nm was observed when these solutions were excited from 290–370 nm. From Fig. 4 it is clear that the fluorescence spectra of cutinase–**4a** and CALB–**4a** (typical data shown for cutinase, dashed line) are similar to that of the free inhibitor **4a** (solid line) in solution, confirming binding of the fluorescent dansyl probe to the proteins. The emission maximum of cutinase–**4a** and CALB–**4a** (at 550 nm) are slightly shifted to higher wavelength (15 nm) as compared to free, unbound **4a**. The curve for CVL–**4a** (dash–dot line) on the other hand is completely different and shows no emission between 460–560 nm when excited at 340 nm. Earlier it was reported by Whitesides *et al.* that the fluorescent signal of a dansyl inhibitor disappeared by binding it in the active site of carbonic anhydrase II. They suggested that surrounding tryptophan residues in the interior of the protein quench the fluorescence of the dansyl group.[19] Therefore, we decided to excite the CVL–**4a** solution at a higher energy wavelength (290 nm) and recorded the fluorescence emission from 400–560 nm (Fig. 4, dotted line). Again free **4a** was measured as a control. Now a clear fluorescent signal was observed with a maximum emission at 470 nm, a significant shift when compared to the maximum emission wavelength of **4a**, cutinase–**4a** and CALB–**4a** (max. em. ~535–550 nm, also when excited at 290 nm). Since we suspected that this enormous shift was due to a reduced polarity surrounding the fluorescent dansyl moiety, we decided to also measure **4a** in various solvents in order to determine how the emission maximum of **4a** shifts going from polar to non-polar solvents. We selected the following solvents with decreasing polarities: 150 mM NH_4OAc buffer, MeCN, CH_2Cl_2 and hexanes. The fluorescent spectra (see ESI for graph†) of **4a** in these solvents clearly revealed that the emission maximum when excited at 290 nm drastically shifts to lower wavelengths when decreasing the polarity of the solvent. Furthermore, a decrease in emission intensity is also observed, a phenomenon similar to what we observed for the CVL–**4a** hybrid as compared to, for example, cutinase–**4a** (Fig. 4). Accordingly, the dansyl fluorescent group is located in the more hydrophobic interior of the CVL protein, which is in agreement with the deep active-site pocket of CVL (*vide supra*). Since the emission maximum of the dansyl moiety in NH_4OAc buffer is hardly shifted for cutinase–**4a** and CALB–**4a** as compared to **4a**, this implies that for these constructs the dansyl group extends outside the protein pocket into the aqueous solution. Again, this is in agreement with the active sites of these proteins being on the protein-surface and thus exposed to the aqueous buffer solution. Clearly, this phenomenon is not unique for PNPPs and therefore such straightforward protocols should be directly transferable to other classes of inhibitors and proteins.

Comparing the fluorescent emission spectra of **4a** and CVL–**4a** at 290 nm excitation (Fig. 4) revealed that CVL–**4a** shows considerable emission at 420–440 nm whereas **4a** shows only minimum emission in that wavelength range and this low emission was found to be independent of the concentration of **4a** (results not shown). This means that the inhibition event of CVL with **4a** can be followed using fluorescence spectroscopy by monitoring the emission increase at 440 nm; only CVL–**4a** shows emission at that wavelength. Therefore, we performed the inhibition experiment as described earlier using 8 equivalents of **4a** with respect to CVL. At time intervals, aliquots of this solution were taken, diluted (10×, final concentration 2.5 μM) with NH_4OAc buffer and the fluorescent emission spectrum at 440 nm was measured (exciting at 290 nm) (Fig. 5). After approximately 30 hours, complete inhibition was obtained and this is in good agreement with the kinetic data obtained from the esterase activity control (*vide supra*). Given the high sensitivity of fluorescence spectroscopy, very low chromophore concentrations can now be measured which allowed us to obtain accurate data for the CVL inhibition event. It was found that CVL inhibition with **4a** followed first order kinetics as well resulting in an accurate inhibition rate constant $k = 0.002\ min^{-1}$.

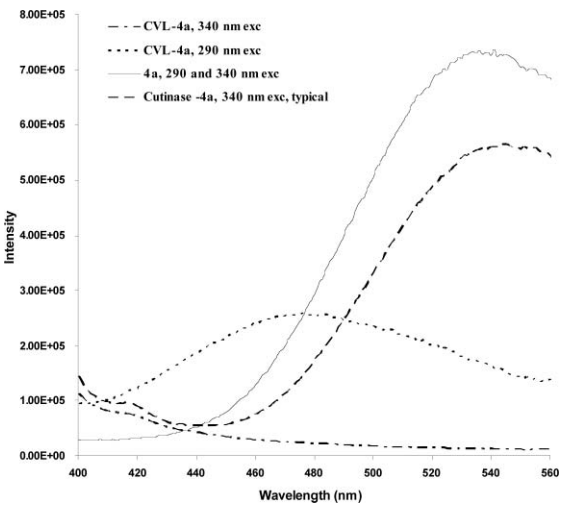

Fig. 4 Fluorescence spectroscopy study of **4a** with various enzymes.

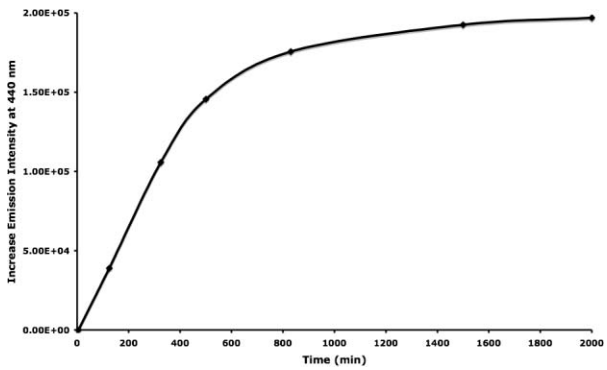

Fig. 5 Inhibition of CVL monitored by fluorescence spectroscopy.

Click reaction on protein

Numerous groups have reported the use of click chemistry to chemically modify biomolecules with special functionalities that can be used for protein diagnosis and profiling.[14] Therefore, we decided to test whether cutinase–**3**, containing an azide functionality, could be functionalised post-inhibition using click chemistry. Mixing cutinase–**3** with propargyl dansylamide in tris–triton buffer pH 8.0 in the presence of $CuSO_4$ (1 mM), tris(benzyltriazole)amine (TBTA, 500 μM), tris(ethylcarboxy)phosphine hydrochloride (TCEP, 1 mM) and sodium dodecylsulfate (SDS, 1%) and incubating the resulting mixture overnight at room temperature, indeed resulted in the formation of a fluorescently labelled cutinase. Successful labelling was determined by analysing the mixture with SDS-PAGE analysis and subsequently exposing the gel to UV-light prior to coomassie blue staining (Fig. 6a + b, respectively). This clearly revealed fluorescently labelled cutinase whereas a control experiment in which $CuSO_4$ was omitted gave no fluorescent labelling of cutinase. This means that our strategy allows both introduction of the desired functionality prior to and after the protein inhibition event, giving an extra dimension to our synthesis design (Scheme 2) and making this strategy very versatile.

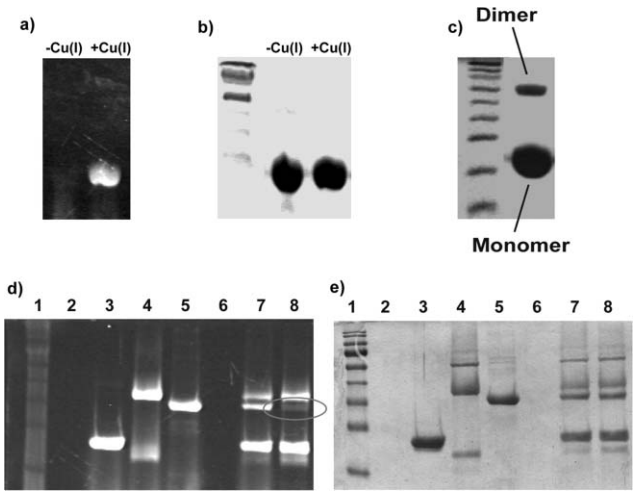

Fig. 6 Protein labelling using reactive phosphonate probes; Click reaction of cutinase–**3** with propargyl dansylamide analysed with (a) UV–Vis and (b) coomassie staining; (c) cutinase dimerisation using PNPP **4c**; protein discrimination using PNPP **4a** and cutinase CALB and CBV analysed with (d) UV–Vis (circle indicates CVL) and (e) coomassie staining.

Another proof of the versatility of our synthesis protocol is the accessibility of bio-probes containing multiple PNP phosphonate functionalities, *e.g.* **4c**. Multivalent bioprobes hold great promise in investigating protein cross-linking and may thus help to understand protein–protein interaction in complex proteomic mixtures.[20] To test whether **4c** can be used for this purpose, **4c** was first reacted with a slight excess of cutinase under the standard inhibition conditions, resulting in cutinase dimer formation (Fig. 6c). Surprisingly, with CALB and CVL no protein cross-linking was observed which is probably due to steric hindrance of the protein; if one of the phosphonate groups is already bound to a protein, the reaction of the second phosphonate group is hampered due to the steric bulk of the protein. Additionally, when **4c** is added to a mixture of all three lipases, only cutinase dimerisation is observed. These results suggest that bifunctional probes such as **4c** may be of interest to investigate (selective) protein–protein interactions in complex proteomic mixtures. This research is currently under investigation.

Selective protein labelling

The significant difference in inhibition rates between cutinase, CALB and CVL with **4a** implies that protein discrimination can be achieved using PNPP probes. To test this hypothesis, we mixed all three proteins in an approximately 1 : 1 : 1 ratio in tris–triton buffer and treated this mixture with both an excess of **4a** and with only 0.3 equivalents of **4a**. After incubating these solutions overnight at room temperature, the resulting mixtures were analysed by SDS-PAGE analysis by exposing the gel to UV-light (Fig. 6d) prior to coomassie blue staining (Fig. 6e) in order to determine fluorescent labelling of proteins. Treating the individual proteins with **4a** resulted in a clear fluorescent spot for all proteins (lanes 3, 4 and 5 for cutinase, CALB and CVL, respectively). Additionally, treatment of the mixture with an excess of **4a** also resulted in the fluorescent labelling of all three proteins (lane 7). However, addition of only 0.3 equivalents of **4a** gave only fluorescent labelling of cutinase and CALB spots (lane 8). Again this is in good agreement with the earlier determined slow inhibition rate of CVL, preventing CVL labelling with **4a** in the latter case. Thus, PNPP probes can discriminate between proteins, even within a subfamily of proteins (lipases).

Moreover, in order to determine the specificity of PNP phosphonate probes for serine hydrolases, we selected a range of proteins from different protein (sub)families possessing various modes of action and incubated them with **4a** as described earlier. Subtilisin, PagP, PagL and patatin are all known serine hydrolases. PagL and patatin are both reported to have esterase activity whereas subtilisin is a hydrolase and PagP an acyl transferase. Treatment of these proteins with **4a** followed by SDS-PAGE analysis revealed fluorescent labelling of all these proteins. Incubating **4a** with members of other protein (sub)families, *i.e.* papain (cysteine hydrolases), bovine serum albumin (BSA), carbonic anhydrase II (carbonate hydrolase), pepsin (aspartic acid protease) and thermolysin (metalloprotease), revealed that PNP phosphonate probes are highly selective for serine hydrolases as no fluorescent labelling of these proteins occurred. These results strongly suggest that PNP phosphonate inhibitors such as **4a** are interesting candidates to selectively label serine hydrolases in complex proteomic mixtures. Initial experiments revealed that **4a** indeed selectively labels proteins in living cells (HeLa cells). Currently, we are optimising these results and are developing proteomic techniques to isolate and analyse the labelled proteins.

Conclusions

We have described a novel and straightforward synthesis protocol for reactive PNPP probes in which the desired tag was introduced in the final step using click chemistry. Both diagnostic (**4a**) and affinity (**4b**) tags could be introduced using this strategy whereas inhibitors containing multiple PNP phosphonate moieties (**4c**) are also available through this methodology. The products are produced in only four steps and since we use a mild click coupling

reaction in the final step it is relatively easy to fine-tune these probes for selected (groups of) proteins by varying the length and nature of the linkers. This strategy should by no means be limited to reactive PNPP probes. The PNPP probes were shown to be selective ABPP inhibitors for serine hydrolases and they can discriminate between proteins, even within a subfamily of proteins (lipases). Because the click reaction is bio-orthogonal we were also able to alter the sequence of events by first inhibiting the enzyme with an azide-functionalised PNP phosphonate inhibitor (**3**) followed by introduction of the diagnostic tag (dansyl group) using click chemistry. This emphasises the flexibility and versatility of our approach. Additionally, we developed easy protocols using UV–Vis and fluorescence spectroscopy to monitor the protein–inhibition event, providing accurate inhibition rate constants for various enzymes and valuable information about the active site (accessibility) of serine hydrolases. Gathering such data is of special importance in ABPP since it gives valuable insight into the factors that influence the protein inhibition event, the crucial step in ABPP. These results illustrate how small organic molecules can serve as diagnostic probes to gather information about the structure and location of the active site of (unknown) proteins. Finally, the high selectivity of our PNP phosphonate probes for serine hydrolases suggests that these probes are ideally suited to selectively label proteins in complex proteomic mixtures, *e.g.* living cells, making them highly interesting for the field of proteomics.

Experimental section

General comments

Organic solvents were dried over appropriate materials and distilled prior to use. All reagents were obtained commercially and used without further purification unless otherwise stated. Triton X-100 was purchased from Serva and tris(hydroxymethyl)-aminomethane from J. T. Baker. Buffer solutions were prepared using Milli-Q grade water. Purification of water (18.2 MΩcm) was performed with the Milli-Q Synthesis system (Millipore; Quantum Ultrapure). ^{1}H, ^{31}P and ^{13}C{^{1}H} NMR spectra were recorded at 298 K on a Varian 400 Spectrometer at 300/400, 75/100 MHz and 162 MHz, respectively, and ^{31}P{^{1}H} NMR spectra were recorded at 298 K on a Bruker AC200 at 81 MHz. All NMR chemical shifts are in ppm referenced to residual solvents (^{31}P{^{1}H} NMR shifts to H_3PO_4). The MALDI-TOF mass spectra were acquired using a Voyager-DE Biospectrometry Workstation (PerSeptive Biosystems Inc., Framingham, Ma, USA) mass spectrometer. Sample solutions with an approximate concentration of 20–30 mg mL^{-1} in CH_2Cl_2 or THF were prepared. The matrix was 3,5-dihydroxybenzoic acid or 9-nitroanthracene with an approximate concentration of 20–30 mg mL^{-1}. A 0.2 μL of the sample and 0.2 μL of the matrix solution were combined and placed on a golden MALDI target plate and analyzed after evaporation of the solvents. Microanalyses were performed by Kolbe, Mikroanalytisches Laboratorium (Müllheim a/d Ruhr, Germany). UV–Vis experiments were performed at room temperature using a Carey-100 spectrometer. Fluorescence spectroscopy was measured on a Spex Fluorolog instrument. Infrared spectra were recorded with a Perkin Elmer Spectrum 1 FT-IR spectrometer. Electrospray ionization mass spectra of the wild-type cutinase and modified cutinase were recorded on a Finnigan LC-Q ion-trap mass spectrometer. All samples were introduced using a nanoflow electrospray source (Protana, Odense, Denmark).

Synthesis of diethyl 2-azidoethylphosphonate (1)[21]. Azide exchange resin on amberlite (32.2 g, 122.36 mmol N_3) was weighed in a 250 mL round bottom flask. Next, DMF (70–80 mL) was added until the suspension could be stirred conveniently. Finally, diethyl-2-bromoethylphosphonate (2.36 mL, 12.0 mmol) was added drowise by means of a syringe. ^{31}P-NMR was used to monitor the conversion of this reaction. After the reaction had reached completion (20 h), the reaction mixture was filtered, and the resin was washed with DMF. Subsequently, the combined DMF-layer was concentrated *in vacuo* and Et_2O (20–30 mL) was added. The mixture was filtered once again and the solid washed with Et_2O. Removal of all volatiles *in vacuo* afforded a yellow oil and this oil was distilled under reduced pressure; yield: 2.62 g, 74%. ^{1}H-NMR (400 MHz, $CDCl_3$): δ 4.09 (m, 4H, P-(O–C*H*$_2$–CH$_3$)$_2$), 3.53 (m, 2H, P–C*H*$_2$–CH$_2$–N$_3$), 2.03 (m, 2H, P–CH$_2$–C*H*$_2$–N$_3$), 1.34 (q, 6H, P-(O–CH$_2$–C*H*$_3$)$_2$). ^{31}P-NMR (162 MHz, $CDCl_3$): δ 27.97 (s).

Synthesis of ethyl 2-azidoethylphosphonochloridate (2). Compound **1** (2.0 g, 9.65 mmol) was weighed in a dry Schlenk tube and Et_2O (30 mL) was added. Next, freshly distilled oxalyl chloride (18.5 mL, 193.0 mmol) was added by means of a syringe. After 10 h at room temperature the reaction was monitored with ^{31}P-NMR, showing full conversion. The reaction mixture was concentrated *in vacuo* to yield a dark brown oil. Due to the sensitivity and toxicity of this compound, the compound was used immediately; yield: 1.81 g, 95%. ^{1}H-NMR (300 MHz, $CDCl_3$): δ 4.30 (m, 2H, P–O–C*H*$_2$–CH$_3$), 3.64 (m, 2H, P–CH$_2$–C*H*$_2$–N$_3$), 2.44 (m, 2H, P–C*H*$_2$–CH$_3$–N$_3$), 1.40 (t, 3H, P–O–CH$_2$–C*H*$_3$). ^{13}C–NMR (100 MHz, $CDCl_3$): δ 16.13 (d, $^{3}J_{P,C}$ = 6.74 Hz, OCH$_2$*C*H$_3$), 33.77 (d, $^{1}J_{P,C}$ = 124.91 Hz, P*C*H$_2$), 45.10 (s, PCH$_2$*C*H$_2$), 64.01 (d, $^{2}J_{P,C}$ = 8.25 Hz, O*C*H$_2$). ^{31}P-NMR (162 MHz, $CDCl_3$): δ 38.7 (s).

Synthesis of ethyl-4-nitrophenyl-2-azidoethylphosphonate (3). Compound **2** was dissolved in dry benzene (40 mL) and a previously prepared solution of 4-nitrophenol (1.27 g, 9.162 mmol) and triethylamine (6.44 mL, 45.81 mmol) in benzene (40 mL) was added dropwise at room temperature. After 3 h of stirring at room temperature, the reaction mixture had turned black. The mixture was concentrated *in vacuo* and subsequently dissolved in Et_2O (150 mL). This solution was washed with 1 M K_2CO_3 (aq) (2 × 100 mL), water (3 × 100 mL), and brine (3 × 100 mL). The organic layer was dried over $MgSO_4$ and concentrated *in vacuo* to yield a yellowish oil. The product was purified by column chromatography (silica gel, Et_2O–hexanes 1 : 4, R_f = 0,16); yield: 1.75 g, 64%. ^{1}H-NMR (300 MHz, $CDCl_3$): δ 8.26 (d, 2H, P–O–Ar*H*–NO$_2$), 7.41 (d, 2H, P–O–Ar*H*–NO$_2$), 4.20 (m, 2H, P–O–C*H*$_2$–CH$_3$), 3.65 (m, 2H, P–CH$_2$–C*H*$_2$–N$_3$), 2.26 (m, 2H, P–C*H*$_2$–CH$_3$–N$_3$), 1.34 (t, 3H, P–O–CH$_2$–C*H*$_3$). ^{13}C-NMR (100 MHz, $CDCl_3$): δ 16.55 (d, $^{3}J_{P,C}$ = 6.03 Hz, OCH$_2$*C*H$_3$), 26.61 (d, $^{1}J_{P,C}$ = 142.10 Hz, P*C*H$_2$), 45.26 (d, $^{2}J_{P,C}$ = 3.02 Hz, PCH$_2$*C*H$_2$), 63.79 (d, $^{2}J_{P,C}$ = 6.74 Hz, O*C*H$_2$), 121.23 (d, $^{3}J_{P,C}$ = 4.53 Hz, Ar*C*), 125.95 (s, Ar*C*), 144.98 (s, Ar*C*–NO$_2$), 155.41 (d, $^{2}J_{P,C}$ = 8.95 Hz, Ar*C*–O). ^{31}P-NMR (162 MHz, $CDCl_3$) δ 25.95 (s). IR (cm^{-1}): 2102 (N$_3$);

anal. calcd. for $C_{10}H_{13}N_4O_5P$: C, 42.26; H, 4.61; N, 19.71; found: C, 42.08; H, 4.55; N, 19.53%.

Typical procedure for the click reaction for the synthesis of dansyl PNPP 4a. This reaction was carried out in a N_2 atmosphere. Azido phosphonate **3** (0.48 g, 1.6 mmol) was dissolved in degassed acetonitrile (5 mL). Next, 2,6-lutidine (0.19 mL, 1.6 mmol) was added, followed by 5-(dimethylamino)-*N*-(prop-2-ynyl)naphthalene-1-sulfonamide[22] (0.46 g, 1.6 mmol). Finally, $[Cu^{I}(CH_3CN)_4PF_6]$ (7.7 mg, 0.0021 mmol) was added. After stirring this solution at room temperature for 24 h, the mixture was concentrated *in vacuo*. The crude product was dissolved in CH_2Cl_2 (10 mL) and this layer was washed with saturated NH_4Cl (aq) (20 mL), H_2 (20 mL) and brine (15 mL). The organic layer was dried ($MgSO_4$) and concentrated giving **4a** as a yellow solid. This solid was washed with hexanes and dried *in vacuo*. Yield: 0.88 g, 93%.

4a. ^{1}H-NMR (400 MHz, acetone-d$_6$): δ 8.54 (d, $^3J_{H,H}$ = 8.40 Hz, 1H, ArH), 8.39 (d, $^3J_{H,H}$ = 8.40 Hz, 1H, ArH), 8.30 (d, $^3J_{H,H}$ = 9.20 Hz, 2H, ArH), 8.23 (d, $^3J_{H,H}$ = 7.20 Hz, 1H, ArH), 7.65 (s, 1H, triazole-H), 7.55–7.62 (m, 2H, ArH), 7.49 (d, $^3J_{H,H}$ = 9.20 Hz, 2H, ArH), 7.26 (d, $^3J_{H,H}$ = 7.60 Hz, 1H, ArH), 7.20 (br. s, 1H, NH), 4.61 (m, 2H, PCH_2CH_2), 4.18–4.24 (m, 4H, $CH_2N + OCH_2$), 2.88 (s, 6H, $N(CH_3)_2$), 2.55–2.66 (m, 2H, PCH_2), 1.28 (t, $^3J_{H,H}$ = 7.20 Hz, 3H, OCH_2CH_3); ^{13}C-NMR (100 MHz, $CDCl_3$): δ 15.89 (d, $^3J_{P,C}$ = 5.83 Hz, OCH_2CH_3), 26.80 (d, $^1J_{P,C}$ = 141.41 Hz, PCH_2), 37.40 (s, CH_2NH), 43.93 (s, PCH_2CH_2), 45.01 (s, $N(CH_3)_2$), 63.91 (d, $^2J_{P,C}$ = 6.64 Hz, OCH_2), 115.41 (s, ArC), 119.63 (s, ArC), 121.64 (d, $^3J_{P,C}$ = 4.53 Hz, Ar*C*), 121.88 (s, ArC), 123.63 (s, ArC), 125.91 (s, Ar*C*), 126.21 (s, ArC), 128.26 (s, ArC), 129.21 (s, ArC), 129.80 (d, $^3J_{P,C}$ = 6.64 Hz, Ar*C*), 130.22 (s, ArC), 130.32 (s, ArC), 136.32 (s, ArC), 144.99 (s, ArC), 151.99 (s, ArC), 155.41 (d, $^2J_{P,C}$ = 7.95 Hz, Ar*C*–O); ^{31}P-NMR (162 MHz, $CDCl_3$) δ 25.00 (s). MALDI-TOF (*m*/*z*): 588.44 (calcd. M^+ : 588.57), 611.36 (calcd. M + Na^+ : 611.57), 627.32 (calcd. M + K^+ : 627.66); anal. calcd. for $C_{25}H_{29}N_6O_7PS$: C, 51.02; H, 5.24; N, 12.62; found: C, 51.10; H, 5.28; N, 12.67%.

4b. ^{1}H-NMR (400 MHz, acetone-d$_6$): δ 8.28 (d, $^3J_{H,H}$ = 8.40 Hz, 2H, ArH), 8.13 (br m, 1H, N*H*–CH_2), 7.98 (s, 1H, triazole-H), 7.47 (d, $^3J_{H,H}$ = 8.40 Hz, 2H, ArH), 6.24 (br s, 1H, NH-biotin), 6.12 (br s, 1H, NH-biotin), 4.77 (m, 2H, PCH_2CH_2), 4.50 (m, 1H, biotin-H), 4.39 (s, 2H, CH_2NH), 4.31 (s, 1H, biotin-H), 4.20 (q, $^3J_{H,H}$ = 6.80 Hz, 2H, CH_2CH_3), 3.17 (m, 1H, CHS), 2.68–2.92 (m, 4H, $CH_2P + CH_2S$), 2.20 (t, $^3J_{H,H}$ = 6.80 Hz, 2H, CH_2CO), 1.70 (m, 2H, CH_2), 1.61 (m, 2H, CH_2), 1.37 (m, 2H, CH_2), 1.25 (t, $^3J_{H,H}$ = 6.80 Hz, 2H, CH_2CH_3); ^{13}C-NMR (100 MHz, $CDCl_3$): δ 17.14 (d, $^3J_{P,C}$ = 5.73 Hz, OCH_2CH_3), 26.79 (s, CH_2-biotin), 28.10 (d, $^1J_{P,C}$ = 141.01 Hz, PCH_2), 29.51 (s, CH_2), 29.69 (s, CH_2), 35.84 (s, CH_2CO), 36.69 (s, CH_2NH), 41.49 (s, CH_2S), 45.29 (s, PCH_2CH_2), 57.05 (s, CHS), 61.57 (S, CH-biotin), 63.09 (S, CH-biotin), 65.20 (d, $^2J_{P,C}$ = 7.04 Hz, OCH_2), 122.95 (d, $^3J_{P,C}$ = 4.53 Hz, Ar*C*), 124.74 (s, ArC), 127.16 (s, ArC), 127.45 (s, ArC), 146.52 (s, ArC), 156.67 (d, $^2J_{P,C}$ = 9.15 Hz, Ar*C*–O), 165.81 (s, NHC(O)NH), 174.98 (s, C(O)NH); ^{31}P-NMR (162 MHz, acetone-d$_6$) δ 27.16 (s). MALDI-TOF (*m*/*z*): 582.54 (calcd. M + H^+: 582.18), 604.47 (calcd. M + Na^+ : 604.17), 620.43 (calcd. M + K^+ : 620.28); anal. calcd. for $C_{23}H_{32}N_7O_7PS{\cdot}(H_2O)_{0.5}$: C, 46.77; H, 5.63; N, 16.60; found: C, 46.94; H, 5.43; N, 16.03%.

4c. ^{1}H-NMR (400 MHz, acetone-d$_6$): δ 8.28 (dd, $^3J_{H,H}$ = 9.20 Hz, $^5J_{H,P}$ = 0.80 Hz, 4H, ArH), 8.02 (s, 2H, triazole-H), 7.49 (dd, $^3J_{H,H}$ = 9.20 Hz, $^4J_{H,P}$ = 1.20 Hz, 4H, ArH), 4.76–4.82 (m, 4H, PCH_2CH_2), 4.59 (s, 4H, OCH_2-triazole), 4.20–4.26 (m, 4H, CH_2CH_3), 3.56–3.63 (m, 12H, 3 × CH_2CH_2O), 2.73–2.82 (m, 4H, PCH_2), 1.28 (t, $^3J_{H,H}$ = 7.60 Hz, 2H, CH_2CH_3); ^{13}C-NMR (100 MHz, $CDCl_3$): δ 15.91 (d, $^3J_{P,C}$ = 5.83 Hz, OCH_2CH_3), 27.11 (d, $^1J_{P,C}$ = 140.51 Hz, PCH_2), 44.04 (s, PCH_2CH_2), 63.42 (d, $^2J_{P,C}$ = 6.64 Hz, OCH_2), 64.35 (s, CH_2), 69.69 (s, CH_2), 70.52 (s, CH_2), 70.57 (s, CH_2), 121.56 (d, $^3J_{P,C}$ = 4.63 Hz, Ar*C*), 123.80 (s, ArC), 125.80 (s, ArC), 144.91 (s, ArC), 145.07 (s, ArC), 155.76 (d, $^2J_{P,C}$ = 7.85 Hz, Ar*C*–O); ^{31}P-NMR (162 MHz, acetone-d$_6$) δ 25.36 (s). MALDI-TOF (*m*/*z*): 827.31 (calcd. M + H^+: 827.25), 849.31 (calcd. M + Na^+: 849.24), 865.27 (M + K^+: 865.35); anal. calcd. for $C_{32}H_{44}N_8O_{14}P_2$: C, 46.49; H, 5.36; N, 13.55; found: C, 46.33; H, 5.30; N, 13.43%.

General protein inhibition experiment

Typically, 10–30 mg of the appropriate enzyme is dissolved in 4.0 mL 0.1% triton, 50 mM Tris buffer at pH 8.0 (acidified with conc. HCl). To 1.0 mL of the protein solution is added 10 μL of a 50 mM solution of **4a** in MeCN and the *p*-nitrophenolate release is monitored by UV–Vis analysis at 410 nm. Alternatively, at certain time intervals, aliquots (typically 100 μL) of the inhibition solution are taken, diluted 10× with 150 mM NH_4OAc buffer and the emission spectra of the resulting solutions at 440 nm (290 nm excitation) are recorded on a fluorescence spectrometer. The rate constants k were obtained by plotting $-\ln(C/C_0)$ against time, where C is concentration residual active (non-inhibited) protein and C_0 is total concentration protein. Activity assay: at certain time intervals (depending on the inhibition rate of the protein), 0.5 μL samples of the protein inhibition solution were taken and added to a 0.25 mM solution of *p*-nitrophenyl butyrate in tris–triton buffer pH 8.0. The rate of *p*-nitrophenolate release was measured using UV–Vis analysis at 410 nm (against a reference sample without protein). Analysing the data revealed a first order inhibition processes. The slow inhibition rate for CVL resulted in a considerable error in the UV–Vis data since the PNP concentration in solution is initially below the detection limit of UV–Vis spectroscopy and gave a high noise to signal ration. Thus no accurate inhibition rate constant could be determined using UV–Vis analysis.

After full inhibition, the protein mixtures were analysed by SDS-PAGE-UV–Vis analysis, fluorescence spectroscopy and/or mass spectrometry. For fluorescence spectroscopy and mass spectrometry, the protein–inhibitor construct was first purified by dialysis against 150 mM NH_4OAc buffer using dialysis cassettes with a Mw cut-off of 10 kDa. Next, the purified protein–**4a** solutions were analysed by fluorescence spectroscopy by exciting the sample at 290 nm and measuring the fluorescent emission from 400–650 nm. For cutinase–**4a** and CALB–**4a** and free **4a** in NH_4Ac (150 mM) buffer, the emission maxima are typically between 550–560 nm whereas for CVL–**4a** the emission maximum lies at 475 nm. For CVL, the inhibition event was monitored by fluorescence spectroscopy by sampling 100 μL aliquots, diluting them 10× with NH_4OAc (150 mM) buffer and measuring the emission intensities at 440 nm (290 nm excitation). The obtained inhibition curve

exhibited first order kinetics, providing an accurate inhibition rate constant for the reaction of CVL with **4a**.

The molecular weights of cutinase–**3**, cutinase–**4a** and cutinase–**4b** in 150 mM NH_4OAc buffer were determined with ESI-MS spectrometry (see ESI†).

Fluorescence spectroscopy of PNP phosphonate probe 4a in various solvents

5 μM solutions of **4a** in various solvents were prepared and their emission spectra from 400–580 nm at 290 nm excitation were measured (see ESI for spectra†). The following solvents were used in decreasing order of polarity: 150 mM NH_4OAc, MeCN, CH_2Cl_2 and hexanes.

Click reaction on cutinase–3 with propargyl dansylamide

To a 125 μM solution of cutinase–**3** (1.0 mL) in 0.1% triton, 50 mM tris buffer at pH 8.0 was subsequently added a 50 mM propargyl dansylamide solution in DMSO (10 μL), a 1.0 mM TCEP solution in H_2O (20 μL), a 100 μL TBTA (tris(benzyltriazolemethyl)amine) solution in DMSO (2.0 μL), a 1% SDS solution in H_2O (10 μM) and a 1.0 mM $CuSO_4$ solution in H_2O (20 μL). The resulting solution was incubated for 12 h at room temperature and the mixture was subsequently analysed by SDS-PAGE and UV–Vis analysis. Finally, the modified protein was purified by dialysis against 150 mM NH_4OAc buffer and analysis by ESI-MS spectrometry revealed the formation of cutinase–**4a** (Mw = 21070 Da).

Acknowledgements

The authors kindly wish to thank C. Versluis and Prof. A. J. R. Heck of the Biomolecular Mass Spectrometry group in the Department of Pharmaceutical Sciences at Utrecht University for measuring the ESI-MS spectra of various protein structures. NRSC-Catalysis is kindly acknowledged for financial support (HPD).

Notes and references

1 C. T. Walsh, S. Garneau-Tsodikova and G. J. Gatto, Jr., *Angew. Chem., Int. Ed.*, 2005, **44**, 2.
2 (*a*) M. P. Washburn, D. Wolters and J. R. Yates, 3rd, *Nat. Biotechnol.*, 2001, **19**, 242; (*b*) S. P. Gygi, B. Rist, S. A. Gerber, F. Turecek, M. H. Gelb and R. Aebersold, *Nat. Biotechnol.*, 1999, **17**, 994; (*c*) E. F. Petricoin and L. A. Liotta, *Curr. Opin. Biotechnol.*, 2004, **15**, 24.
3 G. MacBeath, *Nat. Genet.*, 2002, **32**((Suppl)), 526.
4 D. Rauh and H. Waldmann, *Angew. Chem., Int. Ed.*, 2007, **46**, 826.
5 P. E. Dawson, T. W. Muir, I. Clark-Lewis and S. B. Kent, *Science*, 1994, **266**, 776.
6 (*a*) T. C. Evans, J. Benner, Jr. and M. Q. Xu, *Protein Sci.*, 1998, **7**, 2256; (*b*) T. W. Muir, D. Sondhi and P. A. Cole, *Proc. Natl. Acad. Sci. U. S. A.*, 1998, **95**, 6705.
7 (*a*) H. C. Hang, E.-J. Geutjes, G. Grotenbreg, A. M. Pollington, M. J. Bijlmakers and H. L. Ploegh, *J. Am. Chem. Soc.*, 2007, **129**, 2744; (*b*) L. J. Macpherson, A. E. Dubin, M. J. Evans, F. Marr, P. G. Schultz, B. F. Cravatt and A. Patapoutian, *Nature*, 2007, **445**, 541.
8 M. J. Evans and B. F. Cravatt, *Chem. Rev.*, 2006, **106**, 3279.
9 S. Mahrus and C. J. Craik, *Chem. Biol.*, 2005, **12**, 567.
10 (*a*) G. Zandonella, P. Stadler, L. Haalck, F. Spener, F. Paltauf and A. Hermetter, *Eur. J. Biochem.*, 1999, **262**, 63; (*b*) H. Schmidinger, R. Birner-Gruenberger, G. Riesenhuber, R. Saf, H. Susani-Etzerodt and A. Hermetter, *ChemBioChem*, 2005, **6**, 1776; (*c*) H. Schmidinger, H. Susani-Etzerodt, R. Birner-Gruenberger and A. Hermetter, *ChemBioChem*, 2006, **7**, 527.
11 (*a*) Y. Liu, M. P. Patricelli and B. F. Cravatt, *Proc. Natl. Acad. Sci. U. S. A.*, 1999, **96**, 14694; (*b*) D. Kidd, Y. Liu and B. F. Cravatt, *Biochemistry*, 2001, **40**, 4005; (*c*) N. Jessani, J. A. Young, S. L. Diaz, M. P. Patricelli, A. Varki and B. F. Cravatt, *Angew. Chem., Int. Ed.*, 2005, **44**, 2400.
12 C. A. Kruithof, M. A. Casado, G. Guillena, M. R. Egmond, A. van der Kerk-van Hoof, A. J. R. Heck, R. J. M. Klein Gebbink and G. van Koten, *Chem.–Eur. J.*, 2005, **11**, 6869.
13 A first example in which an organometallic moiety was used as a phasing tool to facilitate the elucidation of a protein crystal structure was recently obtained. These results will be published elsewhere: L. Rutten, B. Wieczorek, J.-P. B. A. Mannie, C. A. Kruithof, H. P. Dijkstra, M. R. Egmond, M. Lutz, A. L. Spek, G. van Koten, P. Gros, R. J. M. Klein Gebbink, *submitted*.
14 (*a*) M. J. Evans, A. Saghatelian, E. J. Sorensen and B. F. Cravatt, *Nat. Biotechnol.*, 2005, **23**, 1303; (*b*) A. Deiters, T. A. Cropp, M. Mukherji, J. W. Chin, J. C. Anderson and P. G. Schultz, *J. Am. Chem. Soc.*, 2003, **125**, 11782; (*c*) A. J. Link and D. A. Tirrel, *J. Am. Chem. Soc.*, 2003, **125**, 11164; (*d*) N. J. Agard, J. M. Baskin, J. A. Prescher, A. Lo and C. R. Bertozzi, *ACS Chem. Biol.*, 2006, **1**, A; (*e*) K. E. Beatty, J. C. Liu, F. Xie, D. C. Dieterich, E. M. Schuman, Q. Wang and D. A. Tirrel, *Angew. Chem., Int. Ed.*, 2006, **45**, 7364; (*f*) J. P. Alexander and B. F. Cravatt, *Chem. Biol.*, 2005, **12**, 1179; (*g*) Q. Wang, T. R. Chan, R. Hilgraf, V. V. Fokin, K. B. Sharpless and M. G. Finn, *J. Am. Chem. Soc.*, 2003, **125**, 3192.
15 T. R. Chan, R. Hilgraf, K. B. Sharpless and V. V. Fokin, *Org. Lett.*, 2004, **17**, 2853.
16 (*a*) C. Jelsch, S. Longhi and C. Cambillau, *Proteins*, 1998, **31**, 320; (*b*) S. Longhi, A. Nicolas, L. Ceveld, M. Egmond, T. Verrips, J. De Vlieg, C. Martinez and C. Cambillau, *Proteins*, 1996, **26**, 442; (*c*) S. Longhi, M. Mannesse, H. M. Verheij, G. H. de Haas, M. Egmond, E. Knoops-Mouthuy and C. Cambillau, *Protein Sci.*, 1997, **6**, 275.
17 (*a*) W. C. Suen, N. Zhang, L. Xiao, V. Madison and A. Zaks, *Protein Eng., Des. Sel.*, 2004, **17**, 133; (*b*) S. Patkar, J. Vind, M. W. Christensen, A. Svendsen, K. Borch and O. Kik, *Chem. Phys. Lipids*, 1998, **93**, 95; (*c*) I. Roy and M. N. Gupta, *Enzyme Microb. Technol.*, 2005, **36**, 896; (*d*) M. R. Castellar, M. A. Taipa and J. M. S. Cabral, *Appl. Biochem. Biotechnol.*, 1997, **61**, 299.
18 The crystal structure data was downloaded from the RSCB Protein Data Base: www.rcsb.org/pdb/home/home.do.
19 A. Jain, S. G. Huang and G. M. Whitesides, *J. Am. Chem. Soc.*, 1994, **116**, 5057.
20 (*a*) T. R. Gadek, *BioTechniques (Suppl.)*, 2003, **34**, 21; (*b*) M. Suchanek, A. Radzikowska and C. Thiele, *Nat. Methods*, 2005, **2**, 261; (*c*) J. T. Ji, *Methods Enzymol.*, 1983, **91**, 580; (*d*) G. Lemercier, S. Gendreizig, M. Kindermann and K. Johnson, *Angew. Chem., Int. Ed.*, 2007, **46**, 4281.
21 We used a modified procedure to literature by exchanging sodium azide with azide-amberlite resin thereby considerably facilitating work-up and purification procedures: D. V. Yashunsky, V. S. Borodkin, M. A. J. Ferguson and A. V. Nikolaev, *Angew. Chem., Int. Ed.*, 2006, **45**, 468.
22 5-(Dimethylamino)-*N*-(prop-2-ynyl)naphthalene-1-sulfonamide was prepared as described: F. Bolletta, D. Fabbri, M. Lombardo, L. Prodi, C. Trombini and N. Zaccheroni, *Organometallics*, 1996, **15**, 2415.